

Effects of the Sintering Temperature on the Structure and Properties of the Alumina Foamed Ceramics

Caiyun JIA¹, Juncheng LIU^{1,*}, Rui DING¹, Dongxiao TENG¹ and Lijie FENG²

¹Shandong University of Technology, Shandong 255049, China

²Zibo Luzhong Refractory Co., Ltd, Shandong 255138, China

Abstract. Alumina foam ceramics reinforced with alumina fibers were prepared with gel-casting. The effects of the sintering temperature on the foam ceramics were investigated. The foam ceramics were composed of α -Al₂O₃, C-AlPO₄, and T-AlPO₄ phases. And the mount of T-AlPO₄ phase decreased, while the mount of C-AlPO₄ phase increased once the sintering temperature exceeded 1180 °C due to the phase transformation of T-AlPO₄ to C-AlPO₄ phase. The grain average size of the foam ceramic increased obviously with the sintering temperature rise, so did its bulk density. While its open porosity decreased. The compression strength of the foam ceramic continuously increased with the sintering temperature rise from 980 to 1580 °C.

Keywords: Foamed ceramics; Alumina; Aluminum hydroxide; sintering temperature.

1 Introduction

Alumina porous ceramic has many unique properties, such as high hardness, high temperature resistance, and erosion resistance etc ^[1-4]. The main materials to form alumina porous ceramics is cheap and easy to get for its rich sources, and the preparation technique is simple. All these imply great commercial value ^[5]. The sintering temperature has great influence on the properties of the foamed ceramics. Delbrücke et al. fabricated porous Al₂O₃ ceramic with porosity of 40.7% and thermal conductivity of 1.63 W/(m·K) by cotton fibers. Samples were sintered at 1600 °C ^[6]. Nait-Ali et al. got ceramic with a porosity of 40~75% and a thermal conductivity 0.8~9 W/(m·K) using polymer as pore-forming agent. Samples were sintered at 1400 °C ^[7]. Shimizu et al. fabricated Al₂O₃ refractory bricks with 90~97.5% porosity by a slurry gelation and foaming method, which were sintered at 1500 °C ^[8]. However, some drawbacks limited the porous ceramic's applications, such as poor shock resistance, and the low strength. The fibers with high modulus and high strength have been

* Corresponding author: jchliu@sdut.edu.cn

used to reinforce the ceramic matrix to prepare composites, called fiber reinforced ceramics matrix composites (FRCMC), which attracted much more attention due to its excellent properties, such as high temperature oxidation resistance, high strength, high elastic modulus, good rigidity, and good chemical stability. The study and application on dense FRCMC have achieved great success^[9-14].

Here was the alumina fiber used to reinforce an alumina foam ceramic, which were prepared with gel-casting. The effects of the sintering temperature on the foam ceramics were investigated.

2 Experiment Procedures

The starting materials included high purity alumina powder (Al_2O_3 , $d_{50}=0.5\mu\text{m}$, 99.99%), H-WF-3 ultra-fine aluminum hydroxide powder ($\text{Al}(\text{OH})_3$, $d_{50} = 3.16\mu\text{m}$, 64.9% alumina), OP emulsifier (with HLB value 14.5), polycrystalline alumina fibers (97% alumina), and aluminum dihydrogen- phosphate ($\text{Al}(\text{H}_2\text{PO}_4)_3$) solution (60 wt%).

The alumina powder, the aluminum hydroxide powder, the OP emulsifier, and the alumina fiber were added into aluminum dihydrogen phosphate solution sequentially to form a mixture. After stirring for 3-5 minutes, PVA powder (as a foam stabilizer) was add into the mixture, and then the deionized water was added to adjust the mixture viscosity, so a slurry came into being. The slurry was then stirred for 2-3h to form uniform foam, till the slurry volume increased no longer. The slurry was casted into disc-shaped mold with diameter of 13.5 cm, standing for 24 h for the sol's gelling at room temperature. The green body was oven-dried at 50 °C for about 2 days, and then sintered at high temperature for 4h with a heating rate of 10°C/min from the room temperature to the set temperature.

The phase compositions of the sintered specimens were analyzed with X-ray diffractometer (XRD, D8 Advanced, Bruker; Cu-K α , 40KV). The micro structures were observed with scanning electron microscopy (SEM, FEI Sirion 200, FEV). Their compression strengths were tested with an electronic universal tester. Their open porosities and bulk densities (D_b) were measured by the Archimedes method. Their conductivities were measured with THQDC-1 type thermal conductivity detector. The slurry viscosity was examined by a rotational viscometer.

3 Results and Discussion

3.1 Effect of the Sintering Temperature on the Phase Compositions

In the sintering process, Al_2O_3 , $\text{Al}(\text{OH})_3$ and $\text{Al}(\text{H}_2\text{PO}_4)_3$ can react each other as the following equations:

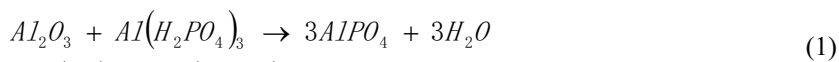


Figure 1 shows the XRD patterns of the specimens sintered at different sintering temperatures. It could be seen that the sintered sample was composed of α - Al_2O_3 、C- AlPO_4 and T- AlPO_4 .

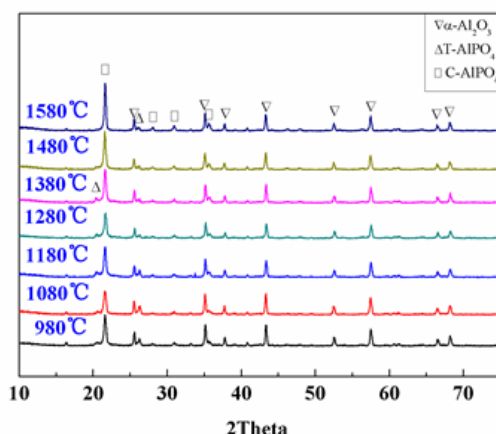


Figure 1 The effect of the sintering temperature on XRD patterns of the specimens

It was worth noting that the peak intensity of C-AlPO₄ phase increased with the sintering temperature increase. On the contrast, the peak intensity of T-AlPO₄ phase decreased, and that of α -Al₂O₃ phase almost kept a constant. One reason should be that the crystallinity of T-AlPO₄ phase improved as the sintering temperature rose. Another reason might be attributed to the phase transformation of T-AlPO₄ to C-AlPO₄ phase occurred at 1219 °C [12].

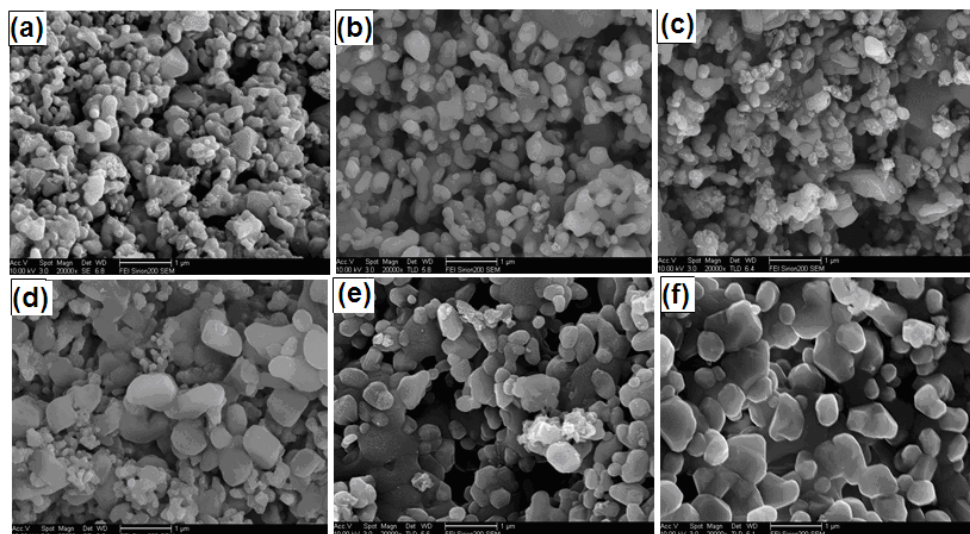


Figure 2 The effect of the sintering temperature on the specimens' microstructure (20000×)

(a) 980; (b) 1080°C; (c) 1180°C; (d) 1380°C; (e) 1480°C; (f) 1580°C.

3.2 Effect of the Sintering Temperature on the Foam Ceramic Microstructure

Figure 2 shows the micro structures of the specimens sintered at different temperature. In general, the average grain size increased with the sintering temperature increase. However, there was a mutation of the grains' morphology and average size between figure 2(c) and 2(d). And it seemed that the microstructure in figure 3(d) was more compact than that in figure 3(c). In figure 2(a) to 2(c), the fine grains dominated the micro structure visual field,

while the fine grains and the coarse ones were half each. And the coarse grains dominated the micro structure visual field in figure 3(e) and 3(f).

3.3 Effect of the Sintering Temperature on the Surface Morphology of the Embedded Fibers

Figure 3 show the microstructures of the fibers embedded in foam ceramics sintered at 1180°C, 1380 °C, and 1580 °C, respectively. Seen from figure 3(a), both the end surface and the cylinder surface of the fiber were clean and smooth. This means that the sintering at 1180°C damaged little the alumina fibers. In figure 3(b), the fiber's surface became a little rough. The end surface roughness increased further, and even the cylinder surface was already indistinct in figure 3(c). It was clear that the sintering at 1380 °C or higher temperature would degrade the fiber in a great deal. The α - Al_2O_3 grains in the fiber would coarsen, and even react with other phases at such a high temperature.

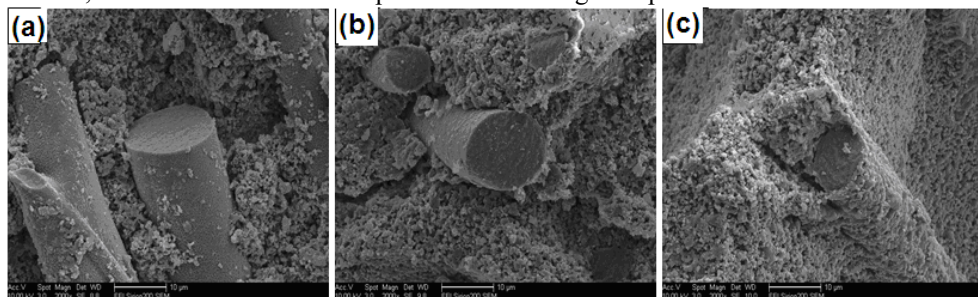


Figure 3 The effect of fibers microstructure in different temperature($\times 2000$)

3.4 Effect of the Sintering Temperature on the Foam Ceramic Properties

In figure 4, the open porosity of the foam ceramic decreased from 82.47% to 74.92% with the sintering temperature rise, while its bulk density increased. As the sintering temperature increased, the grains were easier to grow up, the tiny grains were easier to merge each other, and the grains easier to reassemble. This could be confirmed by figure 2. Therefore, the open porosity reduced.

The compression strength as a function of the sintering temperature is shown in figure 5. It is clear that the compression strength continuously increased with the sintering temperature rise, which could be attributed to the porosity's decrease and the bulk density's increase.

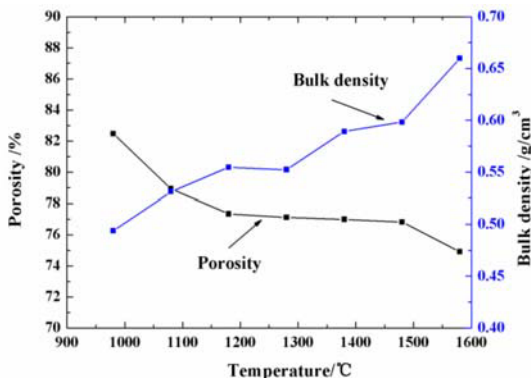


Figure 4 The effect of the sintering temperature on the porosity and the bulk density of the foam ceramic

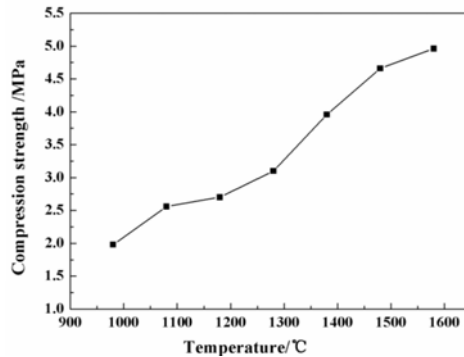


Figure 5 The effect of the sintering temperature on the compression strength of the foam ceramic

4 Conclusions

Alumina foam ceramics were prepared with gel-casting, in which high-purity alumina powder was taken as the main material, aluminum dihydrogen phosphate as the adhesive agent, $\text{Al}(\text{OH})_3$ as the accelerator, and alumina fibers as the reinforcing agent. The effects of the sintering temperature on the foam ceramics were investigated.

(1) The foam ceramics were composed of $\alpha\text{-Al}_2\text{O}_3$, C- AlPO_4 , and T- AlPO_4 phases. And the amount of T- AlPO_4 phase decreased, while the amount of C- AlPO_4 phase increased once the sintering temperature exceeded 1180°C due to the phase transformation of T- AlPO_4 to C- AlPO_4 phase.

(2) The grain average size of the foam ceramic increased obviously with the sintering temperature rise, so did its bulk density. While its open porosity decreased.

(3) The compression strength of the foam ceramic continuously increased with the sintering temperature rise from 980 to 1580°C .

Acknowledgements

This work was financially supported by Project on independent innovation and achievements transformation of Shandong province, Grant No. 2014ZZCX01402.

References

1. R Gaza, E G Yukihara, S.W.S Mckeever. The response of thermally and optically stimulated luminescence from Al_2O_3 : C to high-energy heavy charged particles, *Radiation Measurements* 38 (2004): 417-420.
2. T. Dai, X.M. Guo, Pei, Effects of MCAS glass additives on dielectric properties of $\text{Al}_2\text{O}_3\text{-TiO}_2$ ceramics, *Mater. Sci. Eng. A* 475 (2008): 76-80.
3. L.Y. Shen, M.J. Liu, X.Z. Liu, Thermal shock resistance of the porous $\text{Al}_2\text{O}_3/\text{ZrO}_2$ ceramics prepared by gel casting, *Mater. Res. Bull.* 42 (2007): 2048-2051.
4. M. Gonzalez, E.R. Hodgson, Electrical and mechanical behavior of improved platinum on ceramic bolometer, *Fusion Eng. Des.* 82(2007): 1277-1281.

5. M. Wang, J.B. Wang, Research progress of porous alumina ceramics, *App. Chem. Industry*, 42 (2013): 1505-1507.
6. T. Delbrücke, R.A. Gouvêa, M.L. Moreira, C.W. Raubach, J.A. Varela, E. Longo, Sintering of porous alumina obtained by biotemplate fibers for low thermal conductivity applications, *J. Eur. Ceram. Soc.* 33 (2013) 1087–1092.
7. B. Nait-Ali, K. Haberkö, H. Vesteghem, J. Absi, D.S. Smith, Preparation and thermal conductivity characterisation of highly porous ceramics, *J. Eur. Ceram. Soc.* 27 (2007) 1345–1350.
8. T. Shimizu, K. Matsuura, H. Furue, K. Matsuzak, Thermal conductivity of high porosity alumina refractory bricks made by a slurry gelation and foaming method, *J. Eur. Ceram. Soc.* 33 (2013) 3429–3435.
9. Y.L. Wang, J.J. Hao, Z.M. Guo, Study on the influencing factors of green strength by Gelcasting, *J. Mater. Sci. Eng.* 25 (2007): 262-264.
10. S.H. Lee, W. Markus, A. Fritz, Fabrication of fiber-reinforced ceramic composites by the modified slurry infiltration technique, *J. Am. Ceram. Soc.* 90 (2007): 2657-2660.
11. C.H. Michael, D. James, C. McGuffin, Oxidation kinetics and stress effects for the oxidation of continuous carbon fibers within a microcracked C/SiC ceramic matrix composite, *J. Am. Ceram. Soc.* 91 (2008): 519-526.
12. E.E. Boakye, R.S. Hay, M.D. Petry, T.A. Parthasarathy, Zirconia-silica-carbon coatings on ceramic fibers, *J. Am. Ceram. Soc.* 87 (2004): 1967-1976.
13. S.M. Goushegir, P.O. Guglielmi, J.G. da Silva, M.P. Hablitzel, D. Hotza, H.A. Al-Qureshi, R. Janssen, Fiber-matrix compatibility in an all-oxide ceramic composite with RBAO matrix, *J. Am. Ceram. Soc.* 95 (2012): 159-164.
14. S.H. Li, H.Y. Du, A.R. Guo, H. Xu, D. Yang, Preparation of self-reinforcement of porous mullite ceramics through in situ synthesis of mullite whisker in fly ash body, *Ceram. Inter.* 38 (2012): 1027-1032.